

# Simple, Real-Time Obstacle Avoidance Algorithm for Mobile Robots

IOAN SUSNEA, VIOREL MINZU, GRIGORE VASILIU

Department of Control Engineering  
University "Dunarea de Jos"  
Galati, Str. Domneasca, 47, 800008,  
ROMANIA

ioan.susnea@ugal.ro , viorel.minzu@ugal.ro, vasiliugrigore3@yahoo.com

**Abstract:** - This paper proposes a novel, reactive algorithm for real time obstacle avoidance, compatible with low cost sonar or infrared sensors, fast enough to be implemented on embedded microcontrollers. We called this algorithm "*the bubble rebound algorithm*". According to this algorithm, only the obstacles detected within an area called "sensitivity bubble" around the robot are considered. The shape and size of the sensitivity bubble are dynamically adjusted, depending on the kinematics of the robot. Upon detection of an obstacle, the robot "rebounds" in a direction having the lowest density of obstacles, and continues its motion in this direction until the goal becomes visible, or a new obstacle is encountered. The performances and drawbacks of the method are described, based on the experimental results with simulators and real robots..

**Key-Words:** - Real-time robot control, obstacle avoidance, reactive algorithm, embedded systems

## 1 Introduction

The ability to detect and avoid obstacles in real time is an important design requirement for any practical application of autonomous vehicles. Therefore, a significant number of solutions have been proposed for this problem. Unfortunately, most of these solutions demand a heavy computational load, which makes them difficult, if not impossible, to implement on low cost, microcontroller based, control structures.

This paper presents the results of a research aimed to develop a new algorithm for obstacle avoidance relying on low cost ultrasonic or infrared sensors, and involving a reasonable level of calculations, so that it can be easily used in real time control applications with microcontrollers.

Besides this introduction, the structure of the present paper is as follows:

Section II contains a brief overview of the existing solutions. This section was introduced in order to facilitate the understanding of the proposed algorithm. However, only reactive algorithms, of comparable complexity are considered in this analysis.

Section III contains a description of the proposed solution, and notes on the actual implementation.

Section IV presents the experimental results used for evaluating the algorithm.

Section V is reserved for conclusions and discussion.

## 2 Brief Overview of the Existing Obstacle Avoidance Algorithms

### 2.1 The Bug Algorithms

The simplest obstacle avoidance algorithm ever described is called "the bug algorithm" [1]. According to it, when an obstacle is encountered, the robot fully circles the object in order to find the point with the shortest distance to the goal, then leaves the boundary of the obstacle from this point (see figure 1).

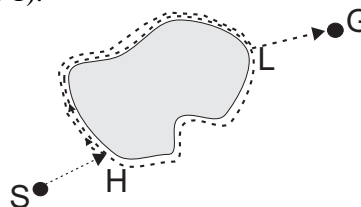


Fig.1 Illustration of the Bug algorithm

This algorithm is obviously very inefficient, and therefore several improvements have been proposed ([2],[3]).

In the 'bug2' algorithm (figure 2), the robot starts following the boundary of the obstacle, but leaves it as soon as it intersects the line segment that connects the start point and the goal.

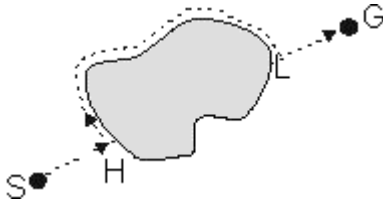


Fig. 2 Illustration of the Bug2 algorithm

Although their simplicity is a major advantage, the bug-type algorithms have some significant shortcomings:

- they do not consider the actual kinematics of the robot, which is important with non-holonomic robots,
- they consider only the most recent sensor readings, and therefore sensor noise seriously affects the overall performance of the robot,
- they are slow.

## 2.2 The Potential Field Algorithm

While the bug-type algorithms are based on a purely reactive approach, the following algorithms tend to view the obstacle avoidance as a sub-task of the path planning, in a deliberative approach.

The potential field algorithm, described in [4], and [5], assumes that the robot is driven by virtual forces that attract it towards the goal, or reject it away from the obstacles. The actual path is determined by the resultant of these virtual forces (see figure 3).

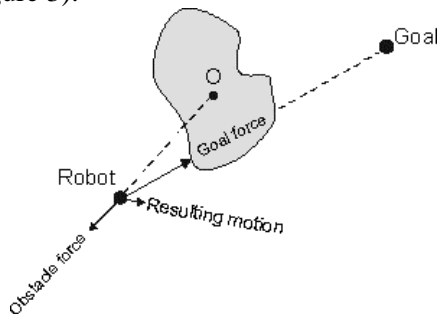


Fig. 3 Illustration of the potential field algorithm

Despite its elegance, this algorithm still does not solve all the drawbacks of the bug algorithms, performs poorly on narrow passages, and is more difficult to use in real time applications.

## 2.3 The Vector Field Histogram (VFH) Algorithm

Described for the first time in [6], and later improved in [7] and [8] by Borenstein et al., the Vector Field Histogram, or VFH algorithm overcomes the problem of the sensors noise by

creating a polar histogram of *several* recent sensor readings, like the one depicted in figure 4.

In figure 4, the x-axis represents the angles associated with sonar readings, and the y-axis represents the probability  $P$  that there really is an obstacle in that direction.

The probabilities are computed by creating a local occupancy grid map of the environment around the robot.

The polar histogram is used to identify all the passages large enough to allow the robot to pass-through. The selection of the particular path to be followed by the robot is based on the evaluation of a cost function, defined for each passage. This depends on the alignment of the robot's path with the goal, and on the difference between the current wheel orientation and the new direction. The passage with the minimum cost is selected.

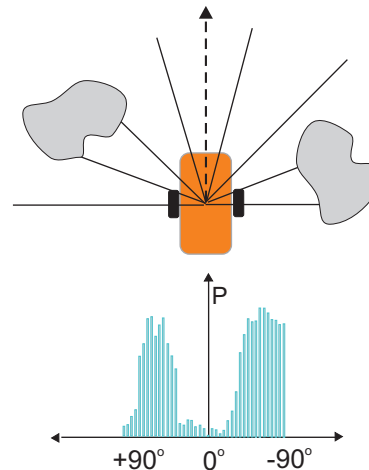


Fig. 4 The polar histogram used in VFH algorithm

This algorithm offers better robustness to sensor noise, and takes into account the kinematics of the robot, but still involves a considerable computation load, which makes it difficult to implement on embedded systems.

## 2.4 The Bubble Band Technique

Proposed by Khatib, and Quinlan in [9], this method defines a "bubble" containing the maximum available free space around the robot, which can be traveled in any direction without collision. The shape and size of the bubble are determined by a simplified model of the robot's geometry, and by the range information provided by the sensors (see figure 5).

With this concept, a *band* of such bubbles can be used to plan a path between a starting point and a goal. Obviously, this technique is more a problem of offline path planning than one of obstacle avoidance, but we have included it in this brief presentation,

because the idea of a bubble, seen as a subset of free space around the robot has some similarity with the solution proposed in this paper.

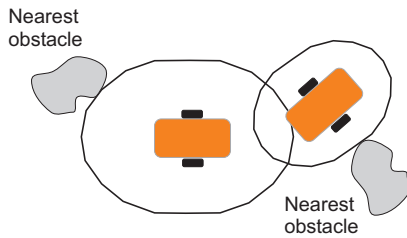


Fig. 5 Illustration of the bubble band concept

### 2.5 Other Obstacle Avoidance Algorithms

There are, of course, several other interesting algorithms for obstacle avoidance. However, relatively few of them are suitable for real-time, embedded applications, and will not be discussed here. Among them, fuzzy logic solutions, like those presented in [10], and [11] can be integrated as a natural extension of the fuzzy path following problem, described in [12].

## 3 Description of the Proposed Solution

### 3.1 Detection of Obstacles

Consider a vehicle, having a ring of equidistant ultrasonic sensors, covering an angle of 180 degrees, as shown in figure 6.

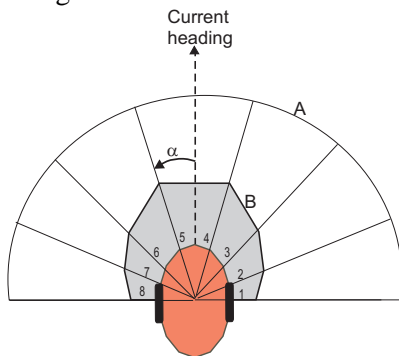


Fig. 6. Robot, ultrasonic sensors, and sensitivity bubble

If  $N$  is the number of sonar sensors, the following code defines the sensitivity bubble:

```

unsigned int sonar_readings[N];
unsigned int bubble_boundary[N];
bubble_boundary[i]=Ki*V*delta_t;
int check_for_obstacles(void){
for(i=0;i<N;i++){
{
if(sonar_readings[i]<=bubble_
boundary[i] return(1);
else return(0);
}
}

```

Where,  $V$  is the translation velocity of the robot,  $delta\_t$  is the time interval between successive evaluations of sensor data, and  $K_i$  are scaling constants, used for tuning. In our experiment,  $K_i \in [0.2 - 3]$ .

Note that the shape and size of the sensitivity bubble (curve B in figure 6) defined like this is dynamically adjusted, depending on the distance that can be traveled through by the robot, during the time interval  $delta\_t$ , provided that the bubble does not exceed the range of the sonar sensors (curve A in figure 6). Also note, that the readings of the sensors represent the distance between the actual position of the sensor (which is on the boundary of the vehicle) and the obstacle. Therefore, the above definition of the sensitivity bubble indirectly includes information on the geometric shape of the robot.

Since the ultrasonic sensors are uniformly distributed, covering an arc of 180 degrees, the sonar readings can be represented in a polar diagram, as shown in figure 7.

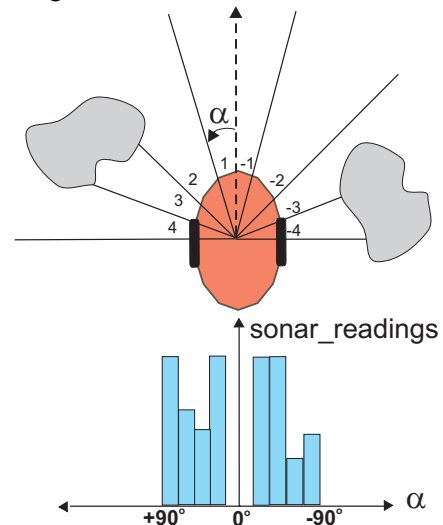


Fig. 7 Polar diagram of the sonar readings

### 3.2 Description of the Algorithm

Initially, the robot moves straight towards the goal. If an obstacle is detected within the sensitivity bubble, the robots “rebounds” in a direction found as having the lowest density of obstacles, and continues its motion in this new direction until the goal becomes visible (i.e. no obstacle within the visibility range of the sonar in that direction), or until a new obstacle is encountered.

Figure 8 presents an illustration of the rebound mechanism. In this image, H is the “hit-point” – the location of the robot at the moment of the detection of an obstacle, and V is the point where the robot

regains visibility of the goal. The whole process is summarized in the flowchart presented in figure 9.

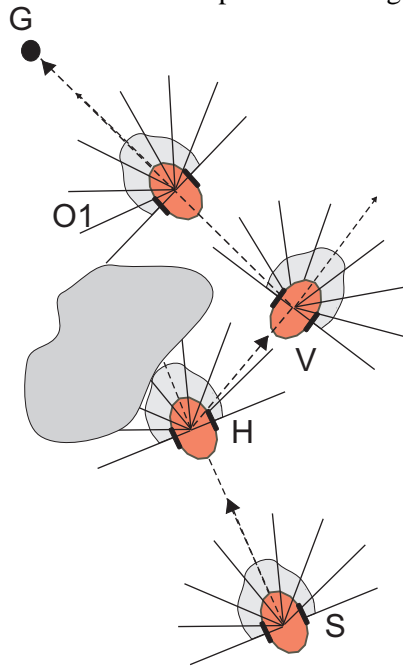


Fig. 8 An illustration of the rebound process

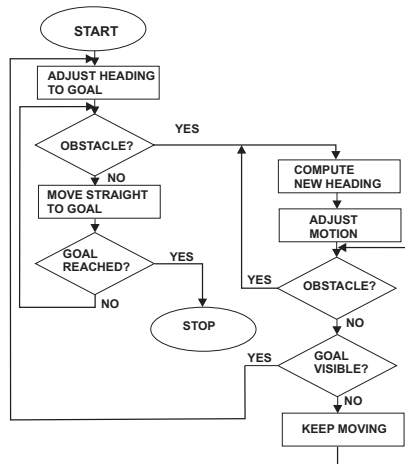


Fig. 9 Flowchart for the bubble rebound algorithm

### 3.3 Computing the Rebound Angle

Considering the fact that the sonar cells are uniformly distributed, at an angular pace:

$$\alpha_0 = \frac{\pi}{N} \quad (1)$$

then, the sonar index,  $i$ , contains angular information:

$$\alpha_i = i\alpha_0$$

$$i \in \left[ -\frac{N}{2}, \frac{N}{2} \right] \quad (2)$$

where  $N$  is the total number of sonar cells. With these notations, the simplest way to compute the rebound angle is:

$$\alpha_R = \frac{\sum_{i=-\frac{N}{2}}^{\frac{N}{2}} \alpha_i D_i}{\sum_{i=-\frac{N}{2}}^{\frac{N}{2}} D_i} \quad (3)$$

where  $D_i$  is the value reported by the sonar cell  $i$ .

## 4 Experimental Results

This experiment is part of a more comprehensive research, aimed to develop cost effective solutions for real time control of mobile robots, based on embedded systems.

The experiment was designed to work with the robots Pioneer3-DX and PeopleBot, manufactured by MobileRobots Inc. ([13]).

During the simulation phase of the experiment, we have used the robot simulator software *MobileSim*, offered by MobileRobots Inc., specifically designed for the Pioneer3 robots.

Various maps of the environment, with multiple distributions of the obstacles were created with the software application *Mapper3*, also from MobileRobots.

The algorithm was also tested using real robots, with satisfactory results.

The actual implementation used a low-cost, 8-bit microcontroller, and was written in C. Besides the obstacle avoidance task, the microcontroller was executing additional tasks for fuzzy path following, and communication, as described in [12].

Figure 10 is a snapshot generated with *MobileSim*, to illustrate the basic obstacle avoidance behavior. Figure 11 shows an example of corridor navigation, and figure 12 shows the trail of the robot while performing a more difficult task, assuming that a higher level global panner, has defined an intermediate goal.

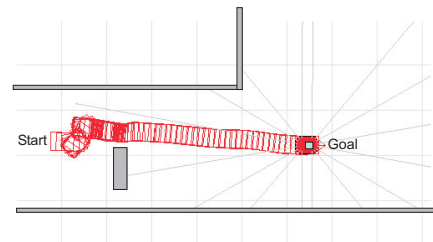


Fig. 10 Basic obstacle avoidance with simulated robot

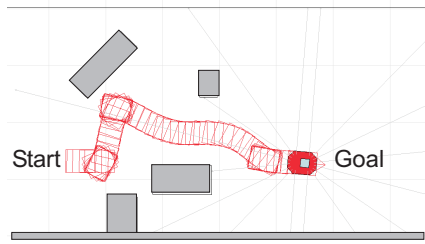


Fig. 11 An example of corridor navigation

Finally, the algorithm was tested with two real robots, namely the models Pioneer3 and PeopleBot of MobileRobots, having the same kinematic model, (see figure 13) in a typical office environment containing a variety of static obstacles, plus human operators moving permanently within the visibility range of the sonars.

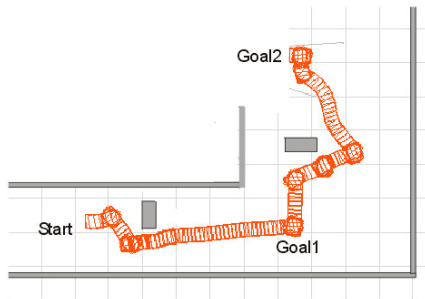


Fig. 12 An example of navigation in maze-type environment, with intermediary goals

The control structure used in the experiment was that described in [14].

The overall performance of the robots in these conditions was satisfactory.

Most of the failures recorded were due to cumulative odometric errors.

The average speed of the robots during the experiments was 0.4m/s, which is reasonable for an intelligent wheelchair, moving indoors.



Fig. 13. The robots used in the experiment

## 5 Discussion

Among the advantages of the proposed solution, we notice:

- It demands very low computational load, and can be implemented on low-cost microcontrollers;
- It is capable to avoid any kind of static obstacles, and even some moving obstacles, like walking humans;
- It requires low cost sensors;
- It can be easily adapted for other sensors, like rotating laser rangefinders;
- It performs very well on narrow corridors.

And the major weaknesses are those common for the majority of purely reactive algorithms:

- It is far from being optimal;
- Like most purely reactive algorithms, it requires a higher level path planner to perform reasonably well in maze-type environments. For example, in figure 12, the algorithm might fail to conduct the robot from Start to Goal2, unless a planner can define intermediary goal Goal1.
- The motion is not smooth;
- Motion is attempted even if there is no path to goal.;
- Failure is possible even when a valid path to goal exists;
- It is still vulnerable to sensor noise. This problem is partly solved with this algorithm because it considers the readings of *all* sensors when computing the rebound angle. However, there is a common situation, presented in figure 14, when sonar sensors fail to detect large obstacles.

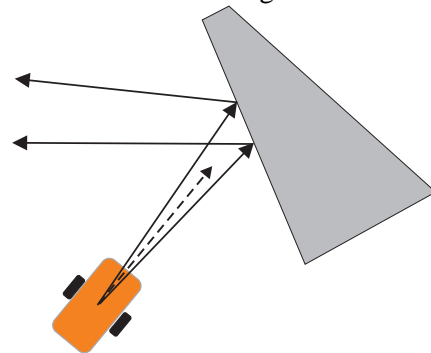


Fig. 14 A common situation when sonar sensors fail

Possible solutions to this problem could be:

- Using a higher density of sensors,
- Using a mix of sonar and infrared sensors for obstacle detection,
- Using a rotating laser sensor.

In principle, the bubble rebound algorithm remains compatible with all of the above mentioned solutions.

Despite the above mentioned drawbacks, the proposed algorithm may be of interest in applications where a higher level path planner is available, and when the cost criterion is particularly important.

Further work is required to improve the overall smoothness of the motion. This is possible, because at this time, the robot stops and adjusts its heading each time an obstacle is detected. Most of the avoidance maneuvers can actually be executed on the fly, without the need to stop the robot.

The experiments with the simulator, and with real robots suggest that such simple algorithms can be used in the implementation of low-cost embedded control devices for intelligent wheelchairs, and other service robots, contributing to a drastic cost reduction of these equipments.

Actually, the algorithm was developed with this type of applications in mind

#### References:

- [1] Lumelsky, V., Skewis, T., "Incorporating Range Sensing in the Robot Navigation Function." *IEEE Transactions on Systems, Man, and Cybernetics*, 20:1990, pp. 1058–1068..
- [2] Lumelsky, V., Stepanov, A., "Path-Planning Strategies for a Point Mobile Automaton Moving Amidst Unknown Obstacles of Arbitrary Shape," in *Autonomous Robot Vehicles*. New York, Spinger-Verlag, 1990
- [3] Kamon, I., Rivlin, E., Rimon, E., "A New Range-Sensor Based Globally Convergent Navigation Algorithm for Mobile Robots," in *Proceedings of the IEEE International Conference on Robotics and Automation*, Minneapolis, April 1996.
- [4] Khatib, O., 1985, "Real-Time Obstacle Avoidance for Manipulators and Mobile Robots." *1985 IEEE International Conference on Robotics and Automation*, March 25-28, St. Louis, pp: 500-505.
- [5] Koren, Y., Borenstein, J., "High-Speed Obstacle Avoidance for Mobile Robotics," in *Proceedings of the IEEE Symposium on Intelligent Control*, Arlington, VA, August 1988, pp: 382-384.
- [6] Borenstein, J., Koren, Y., "The Vector Field Histogram – Fast Obstacle Avoidance for Mobile Robots." *IEEE Journal of Robotics and Automation*, 7, pp: 278–288, 1991.
- [7] Ulrich, I., Borenstein, J., "VFH+: Reliable Obstacle Avoidance for Fast Mobile Robots," in *Proceedings of the International Conference on Robotics and Automation (ICRA'98)*, Leuven, Belgium, May 1998.
- [8] Ulrich, I., Borenstein, J., "VFH\*: Local Obstacle Avoidance with Look-Ahead Verification," in *Proceedings of the IEEE International Conference on Robotics and Automation*, San Francisco, May 24–28, 2000.
- [9] Khatib, O., Quinlan, S., "Elastic Bands: Connecting, Path Planning and Control," in *Proceedings of IEEE International Conference on Robotics and Automation*, Atlanta, GA, May 1993
- [10] Kim J.H., Park J.B., Yang H. "Implementation of the Avoidance Algorithm for Autonomous Mobile Robots Using Fuzzy Rules" in *Fuzzy Systems and Knowledge Discovery*, Springer 2006.
- [11] Tzafestas S.G. and Zavlangas P. Industrial and Mobile Robot Collision-Free Motion Planning Using Fuzzy Logic Algorithms, *Industrial-Robotics-Theory-Modelling-Control*, ARS/pIV, Germany, 2006, pp. 964, 995
- [12] Susnea I, Vasiliu G, Filipescu A, Real-Time, Embedded Fuzzy Control of the Pioneer3-DX Robot for Path Following, *Proceedings of 12<sup>th</sup> WSEAS International Conference on SYSTEMS*, Heraklion, Greece, July 22-24, 2008, pp.334-338,
- [13] [www.mobilerobots.com](http://www.mobilerobots.com)
- [14] Susnea I . Vasiliu G, Filipescu A, Coman G., On the Implementation of a Robotic Assistant for the Elderly. A Novel Approach, *7<sup>th</sup> WSEAS Int. Conf. on Computational, Intelligence Man-machine Systems*, CIMMACS2008